

**Short-range antiferromagnetism in an optimally-doped high  $T_c$   
superconductor**

D. Reznik<sup>1,2</sup>, J.-P. Ismer<sup>3</sup>, I. Eremin<sup>3,4</sup>, L. Pintschovius<sup>1</sup>, M. Arai<sup>5</sup>, Y. Endoh<sup>6</sup>, T. Masui<sup>7</sup>, and S. Tajima<sup>7</sup>

<sup>1</sup>Forschungszentrum Karlsruhe, Institut für Festkörperphysik, Postfach 3640,  
D-76021 Karlsruhe, Germany

<sup>2</sup>Laboratoire Léon Brillouin, C.E.A./C.N.R.S., F-91191-Gif-sur-Yvette  
CEDEX, France

<sup>3</sup>Max-Planck-Institut für Physik Komplexer Systeme, D-01187 Dresden,  
Germany

<sup>4</sup>Institute für Mathematische und Theoretische Physik, TU-Braunschweig,  
38106 Braunschweig, Germany

<sup>5</sup>Institute of Materials Structure Science, KEK, Tsukuba 305-0801, Japan

<sup>6</sup>Synchrotron Radiation Research Center, Japan Atomic Energy Research  
Institute, Hyogo 679-5148, Japan

<sup>7</sup>Department of Physics, Osaka University, Toyonaka, Osaka 560-0043,  
Japan

**High temperature superconductivity occurs in layered copper oxides at  
compositions between undoped insulating and strongly doped  
conventional metallic phases. Some propose that exotic states inherited  
from the antiferromagnetic parent Mott insulators are essential for  
superconductivity<sup>1</sup> whereas others claim that superconductors with the**

**highest transition temperatures,  $T_c$ , conform to the standard model of metals, the Fermi liquid theory<sup>2</sup>. Our neutron scattering experiments on such a superconductor,  $\text{YBa}_2\text{Cu}_3\text{O}_{6.95}$  ( $T_c=93\text{K}$ ), revealed intense magnetic collective modes, which were present both above and below  $T_c$ . They were unexpected from the Fermi liquid theory but similar to spin waves of the parent insulator.<sup>3,4</sup> These modes were very robust and not overdamped indicating anomalously weak coupling to itinerant particle-hole excitations. We conclude that microscopic aggregations of antiferromagnetically-ordered local moments coexist with itinerant electrons even at high doping levels and thus may be intrinsic to all copper oxide superconductors. Weak coupling between spin wave-like excitations of the local moments and the particle-hole continuum points at substantial charge inhomogeneity.**

Magnetic spectra of the copper oxides change dramatically as a function of doping. At  $x=0$ , these compounds are Mott insulators with strong on-site repulsion that localizes electrons whose spins order antiferromagnetically. Their low energy excitations are spin waves (magnons), which disperse upward from the antiferromagnetic (AF) ordering vector<sup>3,4</sup>. Doping disrupts long range AF order, but dispersive excitations similar to magnons remain in underdoped superconductors ( $0 < x < .13$ ) at high energies<sup>5-8</sup>. Their presence implies that AF correlated local moments resulting from Mott physics coexist with metallic bulk properties and superconductivity. Such behavior

falls outside the Fermi-liquid (FL) theory leading to a wide spectrum of exotic theories of high temperature superconductivity. However, the magnon-like modes, which are markers of Mott physics, have not so far been detected in superconductors with  $T_c > 80\text{K}$ . This fact led many to infer that Fermi liquid theory is able to explain superconductivity in copper oxides.<sup>1</sup> Previous experimental studies of the compounds with the highest  $T_{\text{cs}}$  focused primarily on the resonance feature around  $40\text{meV}^{9-11}$  appearing only below  $T_c^{12}$ . Both Fermi liquid and non Fermi liquid scenarios have been proposed to explain the resonance<sup>1,2,5,13-17</sup>.

Here, we focus on magnetic excitations in optimally doped  $\text{YBa}_2\text{Cu}_3\text{O}_{6.95}$  ( $T_c = 93\text{ K}$ ) above  $T_c$  where according to the FL theory, only a broad particle-hole continuum should appear. In order to decide whether this theory can explain the magnetic spectrum or it is necessary to invoke Mott physics, we performed experiments and calculations in absolute units both in the normal and in the superconducting state. Since previous studies failed to clearly distinguish<sup>12,18</sup> the magnetic signal from the nuclear background, we used much longer counting times (more than 1hr/point in some scans) to significantly reduce statistical error. We report that magnon-like modes do exist in  $\text{YBa}_2\text{Cu}_3\text{O}_{6.95}$  in contradiction with the FL prediction (at least in its simple form).

The experiments were performed on the 1T triple-axis spectrometer at the ORPHEE reactor at Saclay utilizing a double focusing Cu111 monochromator and a pyrolytic graphite (PG002) analyzer. The high quality sample of  $\text{YBa}_2\text{Cu}_3\text{O}_{6.95}$  was the same as in an earlier study.<sup>19</sup>

Following Ref. 20, magnetic collective modes were separated from the nuclear background by subtracting spectra recorded at high temperature where the magnetic modes are largely suppressed. Figures 1a and b give examples of the raw data at 52.5 and 60 meV where there is a clear double peak structure around  $h=0.5$ , the AF wavevector of the undoped parent compounds, at 10K and 100K. This feature is suppressed on heating above 300K, as expected from magnetic signal. Some or all intensity that remains at the high temperatures may be magnetic but to be on the conservative side, we subtract the entire high T spectrum divided by the Bose factor from the 10K and 100K data.

The measured energies were chosen to minimize systematic errors due to contamination by nuclear scattering. The biggest error in our experiment is an underestimate of the magnetic signal because some of it (10-20%) may remain at high temperatures where the background was measured. Any broad continuum is indistinguishable from the background and is also not included in the extracted intensities. The observed magnetic signal centered at equivalent antiferromagnetic wavevectors  $\mathbf{Q}=(1.5, 0.5, 1.7)$ ,  $\mathbf{Q}=(0.5, 0.5,$

5.4), and  $\mathbf{Q}=(1.5, 1.5, 1.7)$  in units of  $(2\pi/a, 2\pi/b, 2\pi/c)$ , where (a, b, and c are lattice constants) (data not shown for the latter) agreed with the magnetic form factor confirming the validity of this procedure. (Also see Appendix I) Since YBCO is a bi-layer compound, it shows magnetic excitations of acoustic or optic character. Our choice of  $L=1.7$  and 5.4 selects acoustic magnetic excitations; a separate study will be necessary to investigate optic modes.

Absolute units calibration was performed by comparison with the magnon scattering intensity of insulating  $\text{YBa}_2\text{Cu}_3\text{O}_{6.1}$  (Fig. 2a) already known in absolute units.<sup>4</sup> To correct for sample volume we scaled together spectra of the bond-buckling phonon at  $E = 42.5$  meV, whose eigenvector is unaffected by doping because it does not contain any chain oxygen vibrations.<sup>12</sup> It was measured in identical spectrometer configurations (at  $\mathbf{Q}= 0.5, 0.5, 11$ ) in the two samples. Therefore, no resolution corrections were needed.

Fig. 2 (b-h) shows magnetic spectra of  $\text{YBa}_2\text{Cu}_3\text{O}_{6.95}$  measured at different energies at 10K and 100K, respectively, and Figure 3a,b shows the cut along [1 1 0] after removing effects of the resolution. Similar intensity in constant energy  $\mathbf{q}$ -scans in the [1 1 0] and [1 0 0] directions in Fig. 2 as well as in all previous work indicate that magnetic scattering has a nearly circular symmetry around the reduced antiferromagnetic wave vector  $\mathbf{q}_{\text{af}}=(0.5,0.5)$ , at least in a twinned sample like ours. This makes it easy to integrate the

intensities over  $\mathbf{q}$ . The  $\mathbf{q}$ -integrated magnetic cross section is shown in Figure 4a.

At 100K, we observe a branch above 43 meV dispersing away from  $\mathbf{q}_{\text{af}}$ . Its  $\mathbf{q}$ -integrated intensity is about  $2.2 \text{ m}_b^2/\text{eV}$  and the  $\mathbf{q}$ -width is  $0.3\text{\AA}^{-1}$  full width at half maximum (FWHM), which corresponds to a correlation length of about  $20\text{\AA}$ . Upon cooling to 10K, the scattering intensity at energies below 60 meV increases and a downward-dispersing branch with a constant  $\mathbf{q}$ -integrated intensity of  $6.5\pm1\text{m}_b^2/\text{eV}$  appears between 33 and 41 meV below  $T_c$ . The  $\mathbf{q}$ -width of the lower branch is relatively narrow (Fig. 3a), corresponding to coherent domains of about  $55\text{\AA}$  as demonstrated in Ref. 19. The upward-dispersing branch is significantly less steep than the magnon dispersion in insulating  $\text{YBa}_2\text{Cu}_3\text{O}_{6.1}$ . (Fig. 3a,b) Assuming linear extrapolation, it crosses the zone boundary around 130/100 meV in the  $[1\ 0\ 0]/[1\ 1\ 0]$  direction, respectively, compared with 220meV for the magnons in the insulator. This extrapolation is consistent with recent Raman measurements of 2-magnon scattering.<sup>21</sup> Thus reduced bandwidth of magnetic collective modes compensates the increased spectral weight below 60meV evident from Fig. 4a.

Fig. 3c,d shows the prediction of the FL theory in the standard random phase approximation (FL/RPA),<sup>13-16</sup> using the calculation based on Ref. 16. The

$$\text{RPA expression for the spin susceptibility is: } \chi_{RPA}(\mathbf{q}, \omega) = \frac{\chi_0(\mathbf{q}, \omega)}{1 - g_{\mathbf{q}}\chi_0(\mathbf{q}, \omega)}$$

where  $\chi_0(\mathbf{q}, \omega)$  is the bare susceptibility and  $g_{\mathbf{q}}$  is an electron-electron interaction (four-point vertex), which in general can be momentum dependent<sup>13-16</sup>. Once the parameters of the model were picked to reproduce the known Fermi surface, band width of optimally-doped copper oxides, the superconducting gap<sup>22</sup> and the resonance peak energy there was no further possibility to adjust parameters to alter the calculation results in any significant way. (see Appendix II) Imaginary part of  $\chi(\mathbf{q}, \omega)$  is proportional to the neutron scattering cross section and can be directly compared with experiment. Below  $T_c$  sharp downward-dispersing resonance collective modes appear in the calculation due to an excitonic effect inside the  $d_{x^2-y^2}$ -wave superconducting gap (Fig. 3c)<sup>16</sup>. Above  $T_c$  it predicts only a broad particle-hole continuum and no collective modes (Fig. 3d). Altering momentum dependence of the  $g_{\mathbf{q}}$  does not improve the situation, since it gives wrong resonance peak dispersion.

Reference 20 reported magnetic intensity in slightly underdoped  $\text{YBa}_2\text{Cu}_3\text{O}_{6.89}$  that is remarkably similar to the results of the calculation in Fig. 3c,d. Below  $T_c$  there was a downward-dispersing incommensurate branch below 40meV and a broad commensurate signal centered at the AF wavevector at higher energies. Above  $T_c$ , it reported a very broad magnetic signal just as in the calculation in Fig. 3d. On this basis it has been

concluded that the Fermi liquid theory gives a very good description of the experiment. However, our data at 52.5 and 60 meV, (Figs. 1, 2c,d), which are above the energy range probed in Ref. 20, show clear incommensurate collective modes both above and below  $T_c$  whose dispersion and  $\mathbf{q}$ -integrated intensity was similar to magnons in the parent insulator. (Fig. 3b) FL/RPA does not predict such modes (Fig. 3d), which could only be present if robust short range local moment antiferromagnetism coexisted with the particle-hole continuum.

Such coexistence typically occurs when local and itinerant electrons belong to different bands or different parts of the Fermi surface as, for example, in a heavy-fermion superconductor  $\text{UPd}_2\text{Al}_3$ <sup>23</sup>. In the cuprates, however, it appears within a single band, which is highly anomalous. Furthermore, collective excitations of the local moments should couple strongly to the particle-hole continuum in the normal state and thus be overdamped at least above  $T_c$ .<sup>24</sup> Clear observation of these excitations at 100K implies that this coupling is anomalously weak. One possible reason for the weak coupling is electronic inhomogeneity<sup>25</sup> with the metallic behavior coming from high hole density regions while local moments in low hole density regions order antiferromagnetically. The stripe picture<sup>26,27</sup> is one version of such a scenario (in fact it is consistent with the antiferromagnetic domains of 20 Å), although our results do not prove that it is the only explanation.

Finally we would like to discuss the resonance defined as extra magnetic intensity appearing below  $T_c$ . Going beyond the FL/RPA framework, the excitonic bound state inside the superconducting gap may coexist with the magnon-like branch.<sup>28</sup> Figure 4b compares the increase in the  $\mathbf{q}$ -integrated spin susceptibility from 100K to 10K with the FL/RPA calculation (see Appendix 2). The experimental curve is based on previous detailed studies<sup>19,29,30</sup> with the current investigation contributing the absolute units calibration and the data above 43 meV. The spectral weight of the well known resonance is remarkably well described by the theory. The caveat is that the calculated spectral weight is proportional to the square of the quasiparticle weight,  $Z$ .  $Z$  should be smaller in real systems than in the noninteracting Fermi gas ( $Z<1$ ), but  $Z=1$  in our calculation as well as in Ref. 18. Thus FL/RPA agrees with experiments only to the extent that this assumption is correct. The calculation also does not reproduce the high-energy shoulder, which may originate from local moments whose damping is reduced below  $T_c$ .

To conclude, we find that strong magnetic collective modes unrelated to the particle-hole continuum exist in optimally-doped YBCO and survive the damping expected from this continuum. Thus short-range ordered antiferromagnetic domains weakly coupled to itinerant electrons may be intrinsic to copper oxide superconductors with the highest transition temperatures.

*Acknowledgement:* D.R. would like to thank S.A. Kivelson, J. Zaanen, and M. Vojta for valuable comments on earlier versions of the manuscript. I.E. would like to thank T. Dahm for helpful discussions.

### Appendix I: **Discussion of systematic error**

Systematic errors in the determination of magnetic neutron scattering cross section may result from uncertainty in the nuclear background. Our goal was to measure only magnetic signal peaked in the vicinity of the reduced in-plane wavevector  $\mathbf{q}_{\text{in}}=(0.5,0.5)$ . Thus any background contributions that are  $\mathbf{q}$ -independent or linear in  $\mathbf{q}$  (such as incoherent scattering) may be responsible for statistical error only and do not introduce any systematic error into the extracted magnetic intensities.

The following are the contributions to the nuclear background that may mimic magnetic scattering:

1. Coherent elastic one-phonon scattering may produce peaks when a scan crosses phonon dispersion. One phonon peak intensity as a function of temperature,  $T$ , scales as the Bose factor.
2. Small broad peaks in the background may appear due to coherent multi-phonon scattering. Their intensity increases with  $T$  stronger than the Bose factor.

3. Multiple scattering involving one-phonon and Bragg scattering should produce relatively sharp features in the spectra and its T-dependence follows the Bose factor.
4. Coherent elastic (Bragg) scattering from the sample, which reflects incoherently from either the monochromator or analyzer, produces sharp, often intense, peaks in constant-energy scans. We avoided scans contaminated by any sharp peaks, so it does not contribute to our systematic errors.

We heated the sample above room temperature where  $\mathbf{q}$ -dependent magnetic signal is suppressed, but the nuclear peaks remain. Since most contributions to these peaks scale as the Bose factor, we divided the high temperature scans by the Bose factor and subtracted them from the raw data as illustrated in Fig. 1b,c.

Then the systematic error may only come from differences in the Bose factor corrected nuclear peaks at 300+K and low temperatures, which could be due to:

1. Phonon peaks slightly shifting or broadening in energy with increasing temperature.
2. Peaks due to multiple phonon scattering, which increase with T faster than the Bose factor.

To minimize these errors we performed measurements only at energies where any peaks at  $T > 295\text{K}$  were smaller than the extracted low  $T$  magnetic scattering (with the notable exception of  $35\text{meV}$ , see below). Thus any possible deviations of the  $T$ -dependence of the intensity of the nuclear peaks from the Bose factor due to subtle phonon shifts or multiple phonon scattering were small compared with the final magnetic signal.

For this reason systematic errors due to uncertainty in the nuclear scattering were on the order of 5-10% of the extracted magnetic signal. The  $35\text{meV}$  data are the exception because relatively strong one-phonon scattering could not be avoided there, so the uncertainty in the background is higher as discussed in the caption for fig. 1.

If the high  $T$  data are subtracted without the division by the Bose factor, the linear terms discussed in the caption for Fig. 1c,d become larger, but the extracted magnetic intensity does not change by more than 5%, except at  $35\text{meV}$ , where one-phonon scattering is exceptionally strong. Here the  $100\text{K}$  intensity disappears and the  $10\text{K}$  intensity (shown in Fig. 2e) is reduced by about 20 counts if the Bose factor is not included in the above analysis.

As an independent consistency check, we made sure that the reported magnetic scattering:

1. Obeys crystal symmetry

2. Appears only at small  $Q$
3. Has similar spectral shape and intensity around  $Q=(1.5, 0.5, 1.7)$  and  $(0.5, 0.5, 5.4)$
4. Decreases in intensity with increasing  $T$
5. Was measured only at energies where the nuclear background is nearly featureless to minimize systematic error (except at 35meV)
6. Were consistent with a relatively steep dispersion.

No contamination from nuclear scattering satisfies all these conditions.

## Appendix 2: **Details of the FL/RPA calculation**

A comparison with experiment data can be made via use of the fluctuation-dissipation theorem that relates magnetic scattering cross-section and imaginary part of the transverse spin susceptibility

$$S(\mathbf{q}, \omega) = \frac{\hbar}{\pi} \frac{1}{1 - e^{-\hbar\omega/k_B T}} \text{Im} \chi(\mathbf{q}, \omega).$$

The momentum-integrated energy dependent susceptibility is defined as

$$\chi''(\omega) \equiv \int_{BZ} \chi''(q, \omega) d^3 q.$$

The RPA expression for the spin susceptibility is:

$$\chi_{RPA}(\mathbf{q}, \omega) = \frac{\chi_0(\mathbf{q}, \omega)}{1 - g_q \chi_0(\mathbf{q}, \omega)}, \text{ where}$$

The bare transverse part of the spin susceptibility,  $\chi_0(\mathbf{q}, \omega)$ , is:

$$\chi_0(q, \omega) = \mu_B^2 \sum_k \left\{ \frac{1}{2} \left[ 1 + \frac{\varepsilon_k \varepsilon_{k+q} + \Delta_k \Delta_{k+q}}{E_k E_{k+q}} \right] \frac{f(E_{k+q}) - f(E_k)}{\omega - (E_{k+q} - E_k) + i\Gamma} \right. \\ \left. + \frac{1}{4} \left[ 1 - \frac{\varepsilon_k \varepsilon_{k+q} + \Delta_k \Delta_{k+q}}{E_k E_{k+q}} \right] \frac{1 - f(E_{k+q}) - f(E_k)}{\omega + (E_{k+q} + E_k) + i\Gamma} + \frac{1}{4} \left[ 1 - \frac{\varepsilon_k \varepsilon_{k+q} + \Delta_k \Delta_{k+q}}{E_k E_{k+q}} \right] \frac{f(E_{k+q}) + f(E_k) - 1}{\omega - (E_{k+q} + E_k) + i\Gamma} \right\}$$

where  $E_k = \sqrt{\varepsilon_k^2 + \Delta_k^2}$  is the energy dispersion of the conducting electrons

in the superconducting state with the d-wave superconducting

gap  $\Delta_k = \frac{\Delta_0}{2} (\cos k_x - \cos k_y)$  and the tight-binding energy dispersion

$$\varepsilon_k = -2t(\cos k_x + \cos k_y) + 4t' \cos k_x \cos k_y - 2t''(\cos 2k_x + \cos 2k_y) - \mu \text{ with}$$

the hopping to the nearest, next-nearest and next-next nearest neighbors,

respectively. Here,  $\mu$  is the chemical potential. We employ  $t = 250\text{meV}$ ,

$t' = 0.4t$ ,  $t'' = 0.1t$ , and  $\mu = -1.185t$  to reproduce the known Fermi surface of the

optimally hole-doped cuprates. The antinodal superconducting gap,  $\Delta_0$ , was

chosen to be  $35\text{meV}$ . For given band and superconducting gap parameters

the value of the effective Coulomb interaction

$$g_q = g_0 [1 - 0.3(\cos q_x + \cos q_y)] \text{ at the antiferromagnetic wave vector } \mathbf{Q} \text{ can}$$

be fit to reproduce the resonance condition:

$$1 - g_{\mathbf{Q}} \operatorname{Re} \chi(Q, \omega_{res} = 40\text{meV}) = 0 \text{ which yields } g_0 = 0.5415\text{eV}.$$

A similar calculation in Ref. 21 using a different set of parameters agrees

with very noisy data, but predicts substantial normal state intensity

concentrated within  $0.5\text{\AA}^{-1}$  of  $\mathbf{q}_{af}$  extending down to zero energy. This

intensity is high enough to have been seen in previous experiments (such as in ref.

31) as well as in our experiment, but was never observed.

References:

1. Lee, P. A., Nagaosa, N. & Wen, X.-G. Doping a Mott insulator: Physics of high-temperature superconductivity. *Rev. Mod. Phys.* **78**, 17-85 (2006).
2. Abanov A.r., Chubukov & A.V., Schmalian, J. Quantum-critical theory of the spin-fermion model and its application to cuprates: normal state analysis. *Adv. Phys.* **52**, 119-218 (2003).
3. Tranquada, J. G. Shirane, B. Keimer, S. Shamoto & M. Sato Neutron scattering study of magnetic excitations in  $YBa_2Cu_3O_{6+x}$ . *Phys. Rev. B* **40**, 4503-4516 (1989).
4. Hayden, S. M., Aeppli, G., Perring, T. G., Mook, H. A.& Dogan, F. High-frequency spin waves in  $YBa_2Cu_3O_{6.15}$ . *Phys. Rev. B* **54**, R6905-R6908 (1996).
5. Arai, M. *et al.*, Incommensurate Spin Dynamics of Underdoped Superconductor  $YBa_2Cu_3O_{6.7}$ . *Phys. Rev. Lett.* **83**, 608-611 (1999).
6. Tranquada, J.M. *et al.* Quantum magnetic excitations from stripes in copper oxide superconductors. *Nature* **429**, 534-538 (2004).
7. Hayden, S., Mook, H. A., Dai, Pengcheng, Perring, T. G., Dogan, F. The structure of the high-energy spin excitations in a high-transition-temperature superconductor. *Nature* **429**, 531-534 (2004).
8. Hinkov V. *et al.* In-plane anisotropy of spin excitations in the normal and superconducting states of underdoped  $YBa_2Cu_3O_{6+x}$ . *cond-mat/0601048* (2006).

9. Rossat-Mignod, J. *et al.* Neutron scattering study of the  $\text{YBa}_2\text{Cu}_3\text{O}_{6+x}$  system. *Physica C* **185-189**, 86-92 (1991).
10. He H. *et al.* Magnetic resonant mode in the single-layer high-temperature superconductor  $\text{Tl}_2\text{Ba}_2\text{CuO}_{6+\delta}$ , *Science* **295**, 1045-1047 (2002).
11. Fong H.F. *et al.* Neutron scattering from magnetic excitations in  $\text{Bi}_2\text{Sr}_2\text{CaCu}_2\text{O}_{8+\delta}$ , *Nature* **398**, 588-591 (1999).
12. Fong, H. F. *et al.* Phonon and magnetic neutron scattering at 41 meV in  $\text{YBa}_2\text{Cu}_3\text{O}_7$  *Phys. Rev. Lett.* **75**, 316-319 (1995).
13. Demler, E. & Zhang, S. C. Theory of the resonant neutron scattering of high- $T_c$  superconductors. *Phys. Rev. Lett.* **75**, 4126-4129 (1995).
14. Liu, D. Z., Zha, Y., & Levin, K., Theory of neutron scattering in the normal and superconducting states of  $\text{YBa}_2\text{Cu}_3\text{O}_{6+x}$ . *Phys. Rev. Lett.* **75**, 4130-4133 (1995).
15. Onufrieva, F. & Pfeuty, P., Spin dynamics of a two-dimensional metal in a superconducting state: Application to the high- $T_c$  cuprates, *Phys. Rev. B* **65**, 054515 (2002).
16. Eremin, I., Morr, D. K., Chubukov, A. V., Bennemann, K. H. & Norman, M. R. Novel neutron resonance mode in  $d_x^2-d_y^2$ -wave superconductors. *Phys. Rev. Lett.* **94**, 147001 (2005).
17. Vojta, M., Vojta, T. & Kaul, R. K. Spin excitations in fluctuating stripe phases of doped cuprate superconductors. *Phys. Rev. Lett.* **97**, 097001 (2006).

18 Woo, H. *et al.* Magnetic energy change available to superconducting condensation in optimally doped  $\text{YBa}_2\text{Cu}_3\text{O}_{6.95}$ . *Nature Physics* **2**, 600 (2006).

19. Reznik, D. *et al.* Dispersion of magnetic excitations in optimally doped superconducting  $\text{YBa}_2\text{Cu}_3\text{O}_{6.95}$ . *Phys. Rev. Lett.* **93**, 207003 (2004).

20. Bourges, P. *et al.* The spin excitation spectrum in superconducting  $\text{YBa}_2\text{Cu}_3\text{O}_{6.85}$ . *Science* **288**, 1234-1237 (2000).

21. Hackl, R., private communication.

22 Damascelli, A., Hussain, Z. & Shen, Z.-X. Angle-resolved photoemission studies of the cuprate superconductors. *Rev. Mod. Phys.* **75**, 473-541 (2003).

23. Zwicknagl, G., Yaresko, A., & P., Fermi surfaces and heavy masses in  $\text{UPd}_2\text{Al}_3$ , *Phys. Rev. B* **68**, 052508 (2003)

24. Huang, Z.B., Hanke, W., Arrigoni, E. & Chubukov, A.V. Renormalization of the electron-spin-fluctuation interaction in the t-t'-U Hubbard model. [cond-mat/0603014](https://arxiv.org/abs/cond-mat/0603014).

25. Emery, V.J., & Kivelson, S.A., Frustrated phase separation in copper oxide superconductors, *Physica C* **209**, 597-621 (1993).

26. Zaanen, J. & Gunnarsson, O. Charged magnetic domain lines and the magnetism of high- $T_c$  oxides. *Phys. Rev. B* **40**, 7391-7394 (1989).

27. Machida, K. Magnetism in  $\text{La}_2\text{CuO}_4$  based compounds. *Physica C* **158**, 192 (1989).

28. Segal, I., Prelovšek, P., and Bonča, J. Magnetic fluctuations and resonant peak in cuprates: Towards a microscopic theory. *Phys. Rev. B* **68**, 054524 (2003);

29. Reznik, D. *et al.* Spin Gap in Optimally-doped YBCO. *J. Phys. Chem. Solids* **67**, 509-510 (2006).

30. Fong, H.F., Keimer, B., Reznik, D., Milius, D. L., & Aksay, I. A, Polarized and unpolarized neutron-scattering study of the dynamical spin susceptibility of  $\text{YBa}_2\text{Cu}_3\text{O}_7$ , *Phys. Rev. B* **54**, 6708-6720 (1996).

31. Pailhès, S. *et al.* Resonant Magnetic Excitations at High Energy in Superconducting  $\text{YBa}_2\text{Cu}_3\text{O}_{6.85}$ . *Phys. Rev. Lett.* **93**, 167001 (2004).

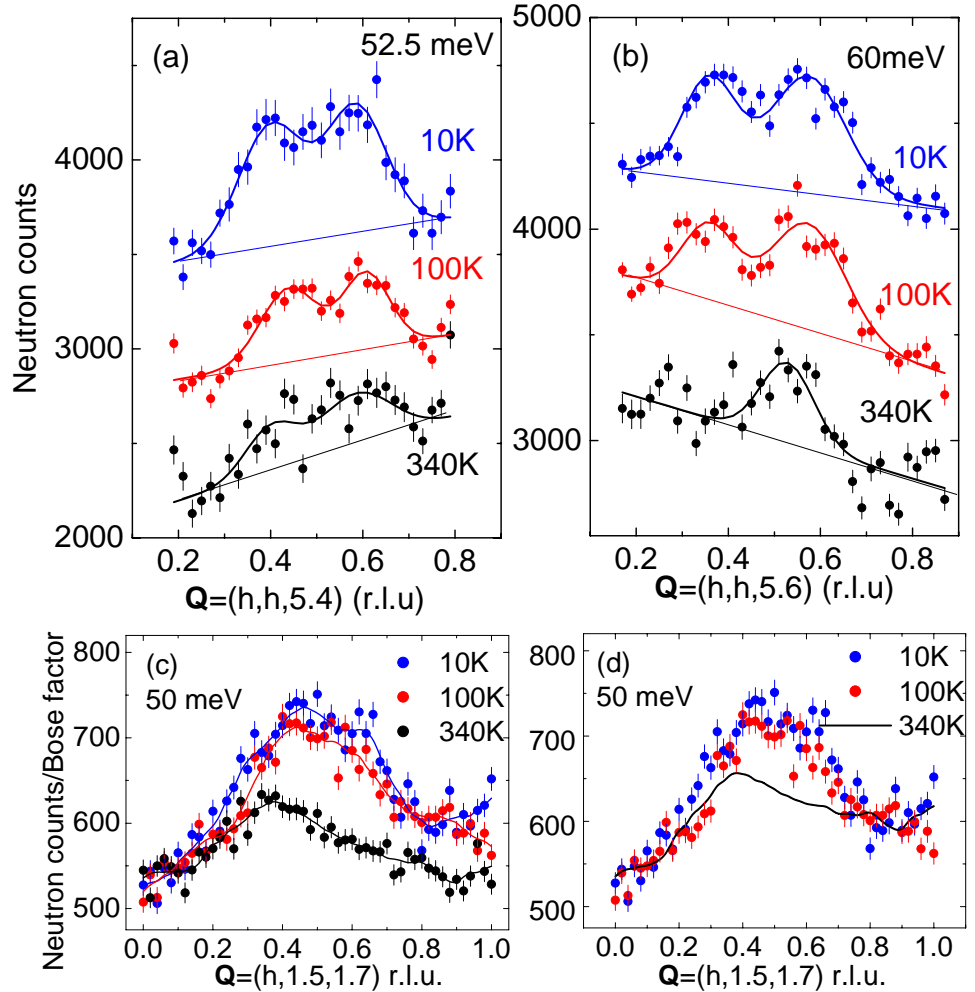


figure 1. Raw data and background subtraction procedure. a,b) Scans at 52.5 and 60meV at 10K, 100K, and 340K offset by a constant for clarity. Lines are guides to for the eye. Note that the peak in (b) at 340K is most certainly nonmagnetic.

c) Scans at 50meV through the antiferromagnetic wavevector divided by the Bose factor. Solid lines represent smoothed data. The feature centered at

$h=0.5$  at 10K and 100K is magnetic because it is suppressed at 330K as the underlying correlations become weaker, leaving behind a “hump” of nuclear scattering peaked at  $h=0.4$ . The background levels near  $h=0$  and  $h=1$  do not exactly match due to small nuclear contributions whose temperature-dependence does not follow the Bose factor (e.g. multiphonon or incoherent elastic nuclear scattering). Linear corrections were added to the 100K and 330K data to match the backgrounds near  $h=0$  and  $h=1$  with the result shown in (b). These corrections were small in all cases (the 50 meV data are the worst case).

d) 50 meV scans after adding the linear terms to the 100K and 330K data. We assign the intensity difference between 10K/100K data and 330K curve to magnetic scattering. Error bars represent s.d.

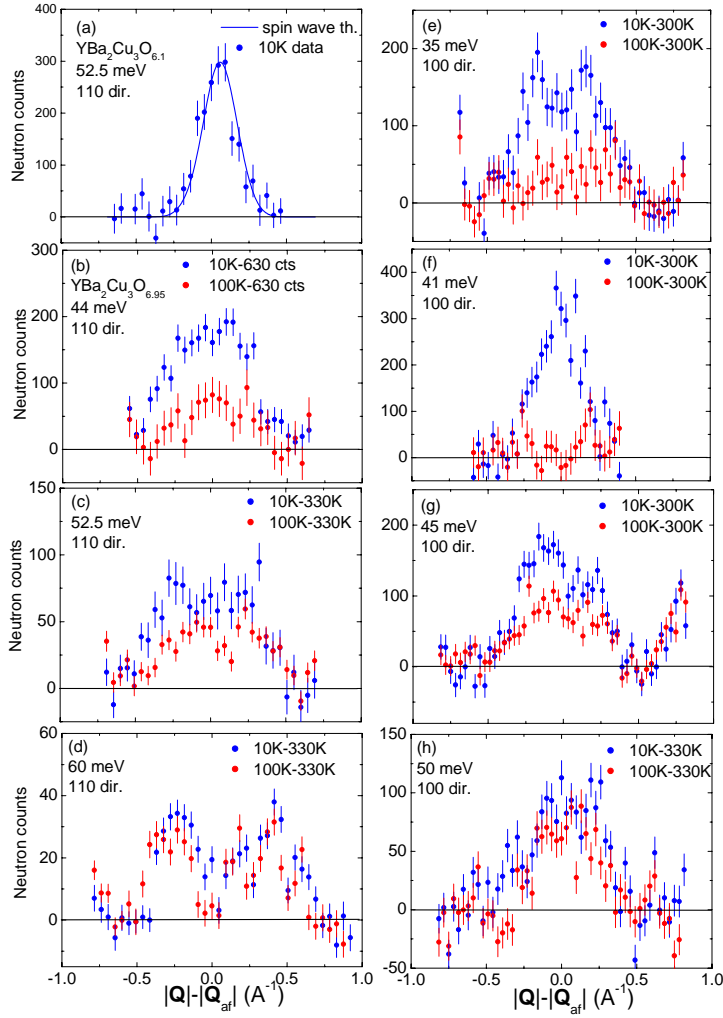


figure 2. Magnetic intensities. a) Magnon peak in  $\text{YBa}_2\text{Cu}_3\text{O}_{6.1}$  at 52.5 meV after subtraction of a flat background. Solid line represents the spin wave model in Ref. 6 convoluted with the spectrometer resolution. b-h) Magnetic scattering in  $\text{YBa}_2\text{Cu}_3\text{O}_{6.95}$  as a function of the distance from the antiferromagnetic ordering wavevector. All spectra have been normalized to the same scale. A constant background of 530 and 630 counts was subtracted

in (a) and (b) respectively, whereas the other magnetic spectra were obtained as described in the text and figure 1. The weak broad 100K signal at 35meV may be an artifact of the background subtraction procedure. Error bars represent s.d.

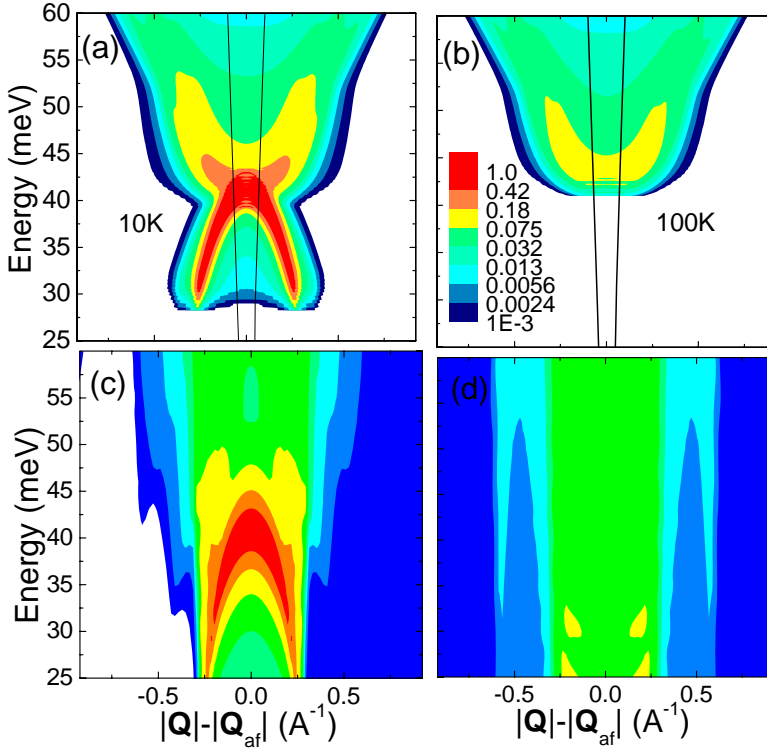


figure 3. Magnetic susceptibility of  $\text{YBa}_2\text{Cu}_3\text{O}_{6.95}$ . a,b) Schematic of the experimentally measured magnetic susceptibility at 10K and 100K in the  $\bar{1}\bar{1}0$  direction after removing effects of the resolution. Different ad. hoc. functional forms were tried until their convolution with the spectrometer resolution agreed with the data. Solid lines represent the magnon dispersion in  $\text{YBa}_2\text{Cu}_3\text{O}_{6.1}$ . c,d) Calculations based on FL/RPA (Ref. 15) for the superconducting state (c) and the normal state (d). Note the logarithmic intensity scale when comparing experimental and calculated spectra.

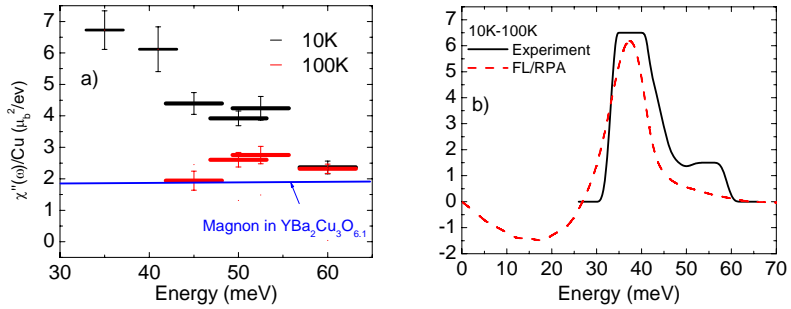


figure 4. **Q**-integrated cross section of magnetic scattering at 10K and 100K in absolute units per spin degree of freedom:  $\chi''(\omega) \equiv \int \chi''(\mathbf{q}, \omega) d^3\mathbf{q}$ . a) The data points represent experimental intensities measured where a clear magnetic signal is observed. The value for the magnon from Ref. 6. was divided by 2 to convert from  $\chi''(\mathbf{q}, \omega)$ /formula unit to  $\chi''(\mathbf{q}, \omega)$ /copper. Vertical error bars represent s.d. only and do not include the possibility that up to 20% of the scattering above 43 meV may be present at 300+K, which was subtracted from the lower T data. Possible inaccuracies in background subtraction (at most 20%) are not included in the error bars. The horizontal width of the symbols represents the s.d. energy resolution. b) The solid line represents the intensity change of the magnetic scattering upon cooling from 100K to 10K in absolute units based on current measurements and previous work.<sup>19,29,30</sup> The sharp low-energy cutoff near 33meV as well as the constant spectral weight between 34 and 41meV were established with high precision<sup>19,29</sup>. The dashed line is a prediction of our FL/RPA calculation.